

Early View

Original article

Quantification of aerosol dispersal from suspected aerosol generating procedures

Runar Strand-Amundsen, Christian Tronstad, Ole Elvebakk, Tormod Martinsen, Marius Dybwad, Egil Lingaas, Tor Inge Tønnessen

Please cite this article as: Strand-Amundsen R, Tronstad C, Elvebakk O, *et al.* Quantification of aerosol dispersal from suspected aerosol generating procedures. *ERJ Open Res* 2021; in press (<https://doi.org/10.1183/23120541.00206-2021>).

This manuscript has recently been accepted for publication in the *ERJ Open Research*. It is published here in its accepted form prior to copyediting and typesetting by our production team. After these production processes are complete and the authors have approved the resulting proofs, the article will move to the latest issue of the ERJOR online.

Copyright ©The authors 2021

Quantification of aerosol dispersal from suspected aerosol generating procedures

Runar Strand-Amundsen¹, Christian Tronstad¹, Ole Elvebakk¹, Tormod Martinsen¹, Marius Dybwad², Egil Lingaas³, Tor Inge Tønnessen^{4,5}

¹ Department of Clinical and Biomedical Engineering, Oslo University Hospital, 0424 Oslo, Norway

² Norwegian Defence Research Establishment (FFI), 2007 Kjeller, Norway

³ Department of Infection Prevention, Oslo University Hospital - Rikshospitalet, 0424 Oslo, Norway

⁴ Department of Anaesthesiology, Division of Emergencies and Critical Care, Oslo University Hospital, 0424 Oslo, Norway

⁵ Institute of Clinical Medicine, Faculty of Medicine, University of Oslo

Correspondence and requests for reprints should be addressed to Runar Strand-Amundsen, PhD, Department of Clinical and Biomedical Engineering, Oslo University Hospital, 0424 Oslo, Norway. Email: runar.strand-amundsen@fys.uio.no

Authors' contributions

RS, CT, OE, TM, MD, EL, TIT designed the study, analysed the results, and wrote and edited the article.

OE included the healthy volunteers. RS, TIT, MD, EL allocated equipment, resources, and facilities. CT performed the statistical analysis. RS, CT, OE, TM performed the experiments. All authors read and approved the final manuscript.

Availability of data and materials

The datasets used and/or analysed during the current study are available from the corresponding author on request.

Abstract

Background:

Oxygen delivering modalities like humidified high-flow nasal cannula (HFNC) and non-invasive positive-pressure ventilation (NIV) are suspected of generating aerosols that may contribute to transmission of disease such as COVID-19. We sought to assess if these modalities lead to increased aerosol dispersal compared to the use of non-humidified low-flow nasal cannula oxygen treatment (LFNC).

Methods:

Aerosol dispersal from 20 healthy volunteers using HFNC, LFNC and NIV oxygen treatment was measured in a controlled chamber. We investigated effects related to coughing and using a surgical facemask in combination with the oxygen delivering modalities. An aerodynamic particle sizer measured aerosol particles (APS3321, 0.3 – 20 μm) directly in front of the subjects, while a mesh of smaller particle sensors (SPS30, 0.3 – 10 μm) was distributed in the test chamber.

Results:

Non-productive coughing led to significant increases in particle dispersal close to the face when using LFNC and HFNC but not when using NIV. HFNC or NIV did not lead to a statistically significant increase in aerosol dispersal compared to LFNC. With non-productive cough in a room without air changes, there was a significant drop in particle levels between 100 cm and 180 cm from the subjects.

Conclusions:

Our results indicate that using HFNC and NIV does not lead to increased aerosol dispersal compared to low-flow oxygen treatment, except in rare cases. For a subject with non-productive cough, NIV with double-limb circuit and non-vented mask may be a favourable choice to reduce the risk for aerosol spread.

Introduction

For COVID-19 patients experiencing reduced lung function with insufficient oxygenation, using humidified High-Flow Nasal Cannula oxygenation (HFNC) and non-invasive ventilation (NIV) have been reported to reduce the frequency of intubation and subsequent invasive mechanical ventilation [1]. HFNC has been associated with a reduction in intensive care unit length of stay [2]. As these treatment modalities are suspected to be aerosol generating procedures [3], some medical centres were initially reluctant to use them and thereby lowered the threshold for intubation. With increasing numbers of COVID-19 patients overwhelming the capacity of ICU beds with invasive ventilation, many patients have been treated in stepdown units with HFNC or NIV. For the health and safety of healthcare workers, it is important to assess to what extent these procedures generate aerosols. Documentation for airborne transmission being a component for the spread of COVID-19 is surfacing [4, 5]. At the same time, there are reports that the potential viral load of aerosolized particles may be low [6].

Several recent approaches have investigated aerosol dispersal and spread during oxygen therapies and research is still ongoing to answer these questions [7-13]. While the present evidence is non-conclusive if HFNC or NIV oxygen treatment has high aerosol dispersal potential, results from recent studies suggests that HFNC and NIV does not lead to significantly increased aerosol dispersal compared to low-flow oxygen modalities [14-17].

In our study aerosol levels were measured in a controlled chamber, where 20 healthy volunteers used HFNC, non-humidified low flow nasal cannula (LFNC), and NIV in BIPAP mode. We investigated the parameter “coughing” with all oxygen modalities, and for HFNC we also investigated using a “surgical facemask”. An aerodynamic particle sizer was used to measure (optical) aerosol particles (0.3 – 20 μm) directly in front (30 cm) of the subject, while smaller optical particle sensors (0.3 – 10 μm) were distributed in the test chamber.

We sought to assess the following questions:

1. Does the use of HFNC or NIV lead to increased aerosol dispersal compared to the use of LFNC?
2. How does non-productive coughing contribute to aerosol dispersal in settings with HFNC/NIV/LFNC?
3. How is the spatial distribution of aerosols in a confined space influenced by HFNC/NIV/LFNC?

Methods

We recruited healthy adult volunteers age >18 years. The recruitment process and study were approved by the regional committee for medical and health research ethics in Norway (approval reference: REK 153325) and written consent was obtained from the subjects.

Experimental protocol

The protocol comprised three oxygen modalities; LFNC, HFNC and NIV (Figure 1B), split into eight events. We included coughing events with all modalities and included a test with a surgical facemask (Medline, EN14683 Type II) within the HFNC modality. The subjects were instructed to provoke coughing (voluntary intensity) every 30 seconds during the coughing tests. To counter potential carryover effects by protocol sequence, the modality order was separated into four differently ordered subsets where the 20 subjects were divided evenly. For LFNC and HFNC we used an Airvo 2 (Fisher & Paykel Healthcare Limited, NZ) with an Optiflow nasal cannula (Fisher & Paykel Healthcare Limited, NZ). The following flowrates were used: LFNC = 4 L/min, HFNC = increments of 10 L/min, starting at 10 and ending at 60 L/min. For NIV (dual-limb) in BIPAP mode (spontaneous, IPAP 10, EPAP 5, support frequency 4) we used a Hamilton C6, (Hamilton Medical, Switzerland) with silicone facial masks (Respireo Hospital F, NonVented disposable).

Test chamber

The test chamber (Figure 1A) with no external active air supply or internal air currents had an internal volume of 11.36 m³ (l:w:h: 234.5 X 234.5 X 206.5 cm), with an anteroom to reduce aerosol contamination. A City M Air Purifier (CAMFIL, USA) with an airflow of 7.2 m³/min was used to zero the particle levels before and between each event. Each subject wore a disposable polypropylene non-woven coverall (Worksafe).

Measurement and equipment

Two different classes of aerosol instruments were used to count and measure particle sizes. A TSI model 3321 Aerodynamic Particle Sizer® (TSI Incorporated, MN, US) was used to sample the air in the breathing-zone 30 cm in front of the subject. Nine small particle sensors (SPS30, Sensirion AG, ZH, Switzerland) were used (custom-made wireless setup) for simultaneous particle counting at different locations (Figure 1A). Both instruments measure the aerosol concentration over a range of particle sizes, from 0.3 µm (optical size) or 0.5 µm (aerodynamic size) to 20 µm for the APS 3321, and from 0.3 µm (optical size) to 10 µm for the SPS30. For readability we use the name “breathing-zone single sensor” for the APS 3321, and “mesh sensors” for the SPS30 sensors.

Prior to performing the experiments, the particle sensors were tested with particle generation from humans and with a NaCl aerosol generator. Temperature and relative humidity in the test chamber were continuously logged during the experiments, with an AM2320 sensor (Guangzhou Aosong Electronics Co., Ltd, China). There was low variation with an average of 26.0 +/- 0.7 STD degrees C and 47.1 +/- 5.6 STD % relative humidity.

Data analysis and statistics

Comparisons were made of the average particle concentration between all pairwise combinations of events relevant to the research questions. As the distributions in concentration values were highly skewed and deviated from a normal distribution (confirmed by Shapiro-Wilk test), comparisons of medians were

conducted. To quantify differences between events, median differences were calculated, and their 95% confidence intervals were estimated using the bootstrap method. The Wilcoxon signed-rank test was used to quantify the statistical significance of the differences. These comparisons were done on both datasets (breathing-zone single sensor and mesh sensors).

To obtain statistical estimates of changes in particle concentration over time, the particle concentration was modelled as a function of time using a linear mixed-effects model with random intercept and slope, using the averaged particle concentrations over each minute as model input. A full covariance matrix based on Cholesky parameterization was used as covariance structure in the models, selected based on the Akaike information criterion on models fit on the breathing-zone single sensor dataset. The particle concentration dependency on the four distance-categories of the mesh sensors (Figure 1A) was modelled statistically for each event using a linear mixed-effects model with random intercept and fixed slope. Estimation of Spearman correlations between emitted particle levels and age, gender and weight were done in Graphpad 9.0.0. All other statistical calculations were done in Matlab R2019b.

Results

Descriptive statistics

20 healthy adult subjects were included in the study, seven were female, mean age was 43 years (11.3 SD) and mean weight 80 kg (18.7 SD). Descriptive statistics for the measurements by the breathing-zone single sensor are presented in Table 1. As visualized in Figure 2 (A, B), there was a large spread in the particle concentration among subjects, with a consistent dispersion around 100% for most events. The distributions were positively skewed with tails of extreme values. Most of the particles measured by the breathing-zone single sensor were in the range of 0.3 – 5 μm (Figure 2E). Our measurement-setup fulfilled the criteria for representative aerosol sampling (intake) and high transport efficiency (tubing) for particle sizes $\leq 5 \mu\text{m}$. The particle dispersal from coughing produced spiked measurements, with the largest spikes attributed to only

a few individuals (Figure 3 and Figures E1-E3). No correlations were found between aerosol dispersion and age, gender, or weight.

Table 1. Descriptive statistics for particles measured in the breathing-zone of the test subject (30 cm from mouth).

Particle size

≤ 1.0 µm:

Event	Mean	Min	Max	Median	0.25	0.75	Dispersion
LFNC	73.0	21.2	151.0	60.9	41.5	106.5	107 %
LFNC+cough	222.7	44.9	1167.4	122.9	71.0	248.4	144 %
HFNC	101.2	15.9	317.1	67.8	38.5	130.0	135 %
HFNC+cough	190.9	36.4	1444.7	91.9	61.8	167.6	115 %
HFNC+M	89.3	25.3	230.5	54.8	41.0	137.2	176 %
HFNC+M+cough	103.1	29.2	270.5	96.7	48.2	156.5	112 %
NIV	77.7	20.6	245.9	66.4	33.3	102.4	104 %
NIV+cough	90.2	28.0	263.5	73.8	39.2	112.2	99 %

Particle size

> 1 µm & ≤ 5 µm:

Event	Mean	Min	Max	Median	0.25	0.75	Dispersion
LFNC	22.1	7.3	70.2	18.6	14.8	24.0	49 %
LFNC+cough	47.3	13.7	242.0	29.3	17.7	40.4	77 %
HFNC	42.4	1.8	236.7	25.7	14.9	46.0	121 %
HFNC+cough	41.8	13.3	186.4	25.0	21.4	37.7	65 %
HFNC+M	33.5	7.6	110.2	22.4	15.4	39.4	107 %
HFNC+M+cough	27.3	8.4	80.1	23.4	17.3	29.1	50 %
NIV	21.6	5.1	51.8	22.1	13.3	26.4	59 %
NIV+cough	24.7	6.0	72.7	21.6	16.3	31.2	69 %

Particle size

> 5µm:

Event	Mean	Min	Max	Median	0.25	0.75	Dispersion
LFNC	1.7	0.5	5.5	1.2	0.9	2.1	100 %
LFNC+cough	1.7	0.3	5.5	1.4	1.0	1.8	57 %
HFNC	3.6	0.1	22.8	1.9	1.2	3.5	122 %
HFNC+cough	3.1	0.6	24.6	1.6	1.1	2.9	113 %
HFNC+M	3.7	0.4	20.5	1.7	1.1	3.9	167 %
HFNC+M+cough	2.6	0.8	9.8	1.9	1.2	2.9	88 %
NIV	1.3	0.3	2.5	1.3	0.9	1.8	65 %
NIV+cough	1.8	0.5	4.5	1.5	1.0	2.2	79 %

Descriptive statistics for the particle concentration (three particle size groups) measured by the breathing-zone single sensor (APS 3321) during all events. The unit used is the mean particle concentration in number per litre during the event. The dispersion of the distribution is presented as the percentwise ratio between the interquartile range and the median. The statistical distributions of particle counts were skewed for nearly all events and particle sizes (Shapiro Wilk $p < 0.05$). LFNC = Low flow nasal cannula, HFNC = High flow nasal cannula, NIV = non-invasive positive-pressure ventilation, M = surgical mask, Swilk = Shapiro-Wilk test.

Inferential statistics

The results from pairwise comparisons of events are shown in Table 2 (breathing-zone single sensor dataset). There was a median increase in particle concentration during HFNC compared to LFNC, but the confidence intervals were wide, including changes in both directions. For particles $> 5\mu\text{m}$, we measured a statistically significant difference between HFNC and LFNC, but the total particle count in this size range was small (median difference 0.5 particles/litre). Comparing events with and without coughing, there was a relatively large increase in particle concentration when coughing during LFNC, and to a lower extent during HFNC. The median particle concentration was lower with HFNC+cough compared to LFNC+cough, but this difference was not statistically significant. Compared to LFNC+cough and HFNC+cough, NIV+cough led to lower levels of particle dispersion, especially in the particle range $\leq 1.0\mu\text{m}$.

Table 2. Statistical pairwise comparisons between events.

Particle size $\leq 1.0\mu\text{m}$:					
Comparison	Median difference	Lower CI	Upper CI	P-value	
HFNC - LFNC	9.5	-5.3	29.6	0.212	
LFNC+cough - LFNC	42.9	8.9	108.5	0.005	
HFNC+cough - HFNC	8.2	-3.4	31.3	0.145	
HFNC+cough - LFNC+cough	-12.1	-59.4	-0.2	0.184	
HFNC - HFNC+M	6.7	-8.5	22.1	0.179	
HFNC+cough - HFNC+M+cough	11.1	-10.9	35.4	0.126	
HFNC+ M +cough - HFNC+ M	2.8	-7.0	14.6	0.332	
NIV - LFNC	-0.7	-4.8	14.2	0.904	
NIV - HFNC	-4.3	-30.3	7.4	0.204	
NIV+cough - NIV	6.6	-14.5	16.0	0.455	
LFNC+cough - NIV+cough	43.4	6.0	94.5	0.001	
HFNC+cough - NIV+cough	28.2	6.4	43.2	0.023	

Particle size > 1 µm & ≤ 5 µm:

Comparison	Median difference	Lower CI	Upper CI	P-value
HFNC - LFNC	6.8	-0.3	16.6	0.073
LFNC+cough - LFNC	7.6	-0.5	16.6	0.048
HFNC+cough - HFNC	1.0	-10.9	5.7	0.765
HFNC+cough - LFNC+cough	-1.4	-7.1	0.0	0.296
HFNC - HFNC+M	2.0	-4.6	13.4	0.391
HFNC+cough - HFNC+M+cough	2.6	-0.4	6.8	0.086
HFNC+ M +cough - HFNC+ M	1.6	-6.6	4.1	0.911
NIV - LFNC	2.5	-4.4	4.4	0.732
NIV - HFNC	-5.5	-20.6	-0.2	0.057
NIV+cough - NIV	2.6	0.0	6.1	0.156
LFNC+cough - NIV+cough	7.1	-2.0	16.0	0.040
HFNC+cough - NIV+cough	4.3	-0.4	11.9	0.107

Particle size > 5µm:

Comparison	Median difference	Lower CI	Upper CI	P-value
HFNC - LFNC	0.5	0.3	0.9	0.044
LFNC+cough - LFNC	0.2	-0.4	0.4	0.862
HFNC+cough - HFNC	-0.5	-0.6	0.1	0.204
HFNC+cough - LFNC+cough	0.3	-0.1	0.9	0.116
HFNC - HFNC+M	0.2	-0.6	0.7	0.926
HFNC+cough - HFNC+M+cough	-0.4	-0.9	0.2	0.125
HFNC+ M +cough - HFNC+ M	0.1	-0.5	0.8	0.709
NIV - LFNC	-0.3	-0.5	0.3	0.468
NIV - HFNC	-0.8	-1.8	-0.2	0.009
NIV+cough - NIV	0.4	0.1	0.8	0.079
LFNC+cough - NIV+cough	-0.2	-0.4	0.3	0.456
HFNC+cough - NIV+cough	0.1	-0.3	0.9	0.390

Statistical pairwise comparisons between different experimental events of particle concentrations [particles per litre of air] measured by the breathing-zone single sensor (APS 3321). Results from three particle size groups are shown. 95% confidence intervals of the median differences are based on the bootstrap method, and the p-values are based on the Wilcoxon signed rank test. LFNC = Low flow nasal cannula, HFNC = High flow nasal cannula, NIV = non-invasive positive-pressure ventilation, M = surgical mask.

Wearing a surgical facemask reduced the mean particle concentration during HFNC, both with and without coughing, but the differences were not statistically significant. Comparing NIV with LFNC, the particle concentrations were similar. None of the mesh sensors measured a statistically significant difference

in particle concentration between HFNC and LFNC. In agreement with the breathing-zone single sensor dataset, the largest differences were attributed to coughing, with the largest effects registered by the sensors near the breathing zone. For details see online supplement (Table E1).

Concentration vs time

Trends over time were close to zero for the events without coughing (Table 3, Figure 3). Although not statistically significant, the estimated trends were largest for LFNC and HFNC with coughing. With HFNC there were typically some early spikes before a slow reduction over time, resulting in slightly negative estimates. For details view Figures E1-E3 (online supplement). The results were similar for the three mesh sensors that were close to the subject (Figure 1, Table E2).

Table 3. Estimates of change in particle concentrations over time.

$\leq 1.0 \mu\text{m}$:

Event	Fixed estimate	Lower 95% CI	Upper 95% CI	Intercept	p-value
LFNC	0.1	-0.5	0.7	72.4	0.721
LFNC+cough	27.3	-4.0	58.6	72.5	0.087
HFNC	-2.5	-6.7	1.7	115.1	0.238
HFNC+cough	25.7	-16.6	68.1	49.4	0.232
HFNC+M	-0.2	-2.2	1.9	90.3	0.862
HFNC+M+cough	4.4	-0.3	9.0	79.0	0.065
NIV	-0.1	-0.7	0.5	78.2	0.743
NIV+cough	3.6	-0.1	7.4	70.2	0.059

$> 1 \mu\text{m} \text{ \& } \leq 5 \mu\text{m}$:

Event	Fixed estimate	Lower 95% CI	Upper 95% CI	Intercept	p-value
LFNC	-0.8	-1.2	-0.5	26.7	<0.001
LFNC+cough	2.4	-4.2	8.9	34.2	0.474
HFNC	-5.8	-13.2	1.5	74.5	0.120
HFNC+cough	-1.2	-8.7	6.3	48.5	0.750
HFNC+M	-2.6	-7.0	1.7	48.0	0.235
HFNC+M+cough	-1.5	-2.9	0.0	35.4	0.049
NIV	-1.2	-1.9	-0.4	28.2	0.002
NIV+cough	0.1	-1.9	2.1	24.2	0.929

$> 5\mu\text{m}$:

Event	Fixed estimate	Lower 95% CI	Upper 95% CI	Intercept	p-value
LFNC	-0.1	-0.2	0.0	2.4	0.009
LFNC+cough	-0.2	-0.3	-0.1	2.7	0.005
HFNC	-0.6	-1.3	0.1	6.7	0.095
HFNC+cough	-0.6	-1.5	0.3	6.4	0.180
HFNC+M	-0.3	-1.1	0.5	5.4	0.440
HFNC+M+cough	-0.3	-0.5	-0.2	4.5	<0.001
NIV	-0.2	-0.3	-0.1	2.5	<0.001
NIV+cough	-0.1	-0.2	0.0	2.3	0.084

Estimates of change in particle concentration (number/litre) per minute near the breathing-zone of the subjects for all events, based on measurements from the breathing-zone single sensor (APS 3321). Results from three particle size groups are shown. LFNC = Low flow nasal cannula, HFNC = High flow nasal cannula, NIV = non-invasive positive-pressure ventilation, M = surgical mask.

Concentration vs distance

With the mesh sensors there were few distance-dependent differences detected except for events involving coughing (Table 4, Figure 4). With coughing, the differences between 30 and 100 cm were small, but the particle concentration was significantly reduced at 180 and 285 cm. Notably for HFNC-M, the particle concentration was lowest at the closest distance but significantly increased 100 cm in front of the subject.

Table 4. *Estimates of differences to intercept (30 cm) in mean particle concentration at different distances in the measurement chamber*

Event	0.3 m (intercept)	1.0 m	1.8 m	2.85 m
LFNC	218.2 (168.0, 268.3)	22.9 (-23.1, 68.8)	-38.0 (-89.4, 13.4)	-14.6 (-79.6, 50.4)
LFNC+cough	400.2 (293.1, 507.3)	-20.3 (-84.2, 43.6)	-102.6 (-174.1, -31.1)*	-100.9 (-191.3, -10.5)*
HFNC	278.1 (219.2, 337.0)	-30.4 (-94.8, 34.0)	-34.8 (-106.8, 37.2)	-16.5 (-107.5, 74.5)
HFNC+cough	341.8 (258.6, 425.0)	7.1 (-53.6, 67.8)	-99.5 (-167.3, -31.7)*	-104.0 (-189.8, -18.2)*
HFNC+M	210.5 (167.2, 253.9)	79.1 (31.5, 126.7)*	14.0 (-39.2, 67.2)	25.0 (-42.3, 92.4)
HFNC+M+cough	303.4 (260.2, 346.7)	-31.0 (-92.2, 30.2)	-57.8 (-126.2, 10.5)	-71.3 (-159.4, 16.8)
NIV	222.8 (183.9, 261.7)	35.3 (-19.8, 90.3)	-30.2 (-91.7, 31.3)	-20.4 (-98.2, 57.42)
NIV+cough	228.4 (181.6, 275.3)	33.8 (-17.5, 85.0)	-43.0 (-100.3, 14.2)	9.7 (-62.6, 82.0)

Estimates of differences in mean particle concentration (number/L) between mesh sensors at different distances from the breathing-zone of the subject based on a linear mixed-effects model. The particle concentration number includes particle sizes (0.3 μ m -10 μ m). The intercept level at 30 cm is presented together with the differences (vs 30 cm) at 100 cm, 180 cm and 285 cm. 95% confidence intervals of all

estimates are given in parentheses, and all differences (vs 30 cm) with a p value < 0.05 are marked with *. LFNC = Low flow nasal cannula, HFNC = High flow nasal cannula, NIV = non-invasive positive-pressure ventilation, M = surgical mask.

Discussion

We investigated the aerosol dispersal from the respiratory tract of 20 healthy adult volunteers in a test chamber with a close to zero particle baseline level, while using LFNC, HFNC or NIV, combined with the parameters “coughing” and “surgical facemask”. The key findings were that HFNC or NIV did not lead to large increases in aerosol dispersal compared to LFNC, except in rare cases (3/20). When investigating changes in particle concentration at different distances, there were no large differences between LFNC, HFNC and NIV.

There was a tendency for small increases in median particles during HFNC compared to LFNC, for the lower particle ranges ($< 5 \mu\text{m}$). Helgeson *et al.* reported a similar non-significant increase at 4 cm from the mouth of the subjects when using HFNC or oxymask. For the particle range $> 5 \mu\text{m}$ we measured a statistically significant difference at 30 cm, but the overall number of particles measured in this range was low, with a median difference of just 0.5 particles per litre (Table 2). The main contribution to this increase came from three subjects that dispersed more particles (of all sizes measured) when using HFNC compared to LFNC (Table 2, Figure 2.C/D), indicating that in rare cases healthcare workers could expect patients connected to HFNC to disperse more particles. Comparing NIV with LFNC, the particle concentrations were similar, indicating that NIV did not lead to increased aerosol dispersal (Table 2, Figure 2.C/D). The mesh sensors dataset showed similar results for pairwise comparisons between events for all sensors (online supplement, Table E1). There was a trend with HFNC with spikes during the first minutes (Figures E1-E3) that could be related to the nasal irritation that some of the subjects (30%) reported during this period. This nasal irritation might explain the slightly higher median with HFNC compared to LFNC.

Our results generally agree with recent studies that indicate that HFNC does not lead to significantly increased aerosol dispersal compared to LFNC in a group of healthy adults [7-9, 11]. The large spread in individual aerosol dispersal among the 20 subjects (Figure 2), despite measures to reduce confounders and background noise, indicates that there are strong individual factors influencing aerosol dispersal. To compare the extremes, the individual with the lowest aerosol dispersal produced 52 particles/L mean for the eight events of the protocol, while the individual with the highest aerosol dispersal produced 425 particles/L mean.

We used a controlled chamber and zeroed particles between each event, to ensure accurate measurement of aerosol dispersal from the subjects without dampening effects from active air circulation. Most of the recent studies have investigated particle dispersion in a negative-pressure room to reduce the ambient background [11, 16, 18], but this does not completely exclude ambient particles that potentially can contribute to the measurements. Wilson *et al.* used zeroing of particle levels between measurements like we did [15].

The airflows used for HFNC and LFNC were similar to what is typically used in the clinic, and to what have been used in recent studies, while our setup with a mesh of sensors in the test chamber was more extensive than other recent studies [11, 14-16, 18]. Gaeckle *et al.* and Wilson *et al.* used funnels to accurately capture all dispersed aerosols, but this approach does not allow for the ability to measure how aerosols spread spatially from the subject. Bem *et al.* measured at the four cardinal directions from the subject during HFNC, capturing particle dispersion in a circle around the subject at 30 cm and 1 meter when using HFNC (60 L/min), but to achieve the spatial resolution they measured eight separate times with a handheld instrument. We measured simultaneously at 10 different locations to the sides and in front of the subject for a distance up to 2.85 meter (Figure 1). Our results corroborate the results reported by Bem *et al.* in that there were no significant differences particle levels between LFNC and HFNC for the particle range below 5 μm [16].

While we found few differences in particle levels vs different distances for LFNC, HFNC and NIV without coughing, we did detect a difference in particle levels as a function of distance for episodes involving coughing. LFNC+cough and HFNC+cough led to relatively large increases in particle concentration close to the subjects (Table 3, Figure 3), indicating how coughing can lead to a build-up of aerosol particles (10-minute period) in an enclosed space with no air circulation, where aerosol concentration drop-off occurred between 100 cm and 180 cm (Figure 4, Table 4). In a hospital setting there will typically be an active room ventilation creating airflows moving in the room. The turbulences formed by these air currents will vary with each location. Consequently, making exact predictions about safe distances are difficult. If the clinical setting involves low air-change rates like in a standard patient room, our results indicate that a clinician treating (LFNC or HFNC) a coughing patient may be exposed to significantly lower particle levels at 180 cm distance compared to a 100 cm distance or closer.

There was a significant reduction in measured particle levels when comparing HFNC+cough or LFNC+cough with NIV+cough, indicating that for a patient with non-productive cough, NIV with double limb circuit and non-vented mask can be a favourable choice to reduce aerosol dispersal. For patients with productive cough, other modalities may be favourable. Gaeckle et al. reported that NIV might have a dampening effect on aerosol dispersal [11]. Wilson *et al.* reported a lower increase in particles when using single-limb NIV compared to dual-limb NIV (we used dual-limb).

Wearing a surgical mask (HFNC+mask+cough) had a dampening effect on the large cough-spikes of particles in the medium ($>1\mu\text{m}$ & $\leq 5\mu\text{m}$) and large ($> 5\mu\text{m}$) particle size range (Figures E2 and E3). As a comparison Wilson *et al.* reported that using a surgical mask halved the number of particles measured in most instances they tested when using HFNC and NIV on 10 healthy volunteers.

Our primary interest was in the $0.3 - 5.0\mu\text{m}$ particle size range (Figure 2E) which are typically the dehydrated remains from slightly larger primary respiratory droplets. While particles in this size range represents only a fraction of the total volume emitted from the respiratory tract and have lower viral load potential than the larger particles, they are emitted in huge numbers compared to the larger particles [19], and can remain airborne for longer periods of time (hours) under all temperature and relative humidity

conditions [20]. At the same time, particles in this range are known as the “breathable/inhalable fraction” and will typically reach and be deposited in the bronchioles and the alveoli of the lower airways [21]. The smallest particle size ($0.3\mu\text{m}$) in the range we measured (Figure 2E), is known as “the most penetrating particle size” due to the difficulty of capturing this particle size with particle filters [22].

Limitations

This was an explorative study, where the effect sizes and individual variations were unknown prior to the study. Due to the large individual variation, the study sample size ($n=20$) may have limited the power to detect true differences between groups. For future studies we recommend including a larger number of subjects to better account for individual variation. Patients with respiratory disease might have changes in airway parameters, resulting in different aerosol generation characteristics than from healthy adult subjects [23]. Thus, our results might underestimate aerosol dispersal compared to people affected by respiratory disease. Our results in a controlled chamber might not apply for a clinical setting, where room ventilation frequencies and sizes are different.

Provoked coughing by healthy adults may be a poor representation of actual aerosol dispersal by patients that have airway related diseases. Also, there was large individual variation in coughing intensity. Although the measurements of the low-cost mesh sensors tended to agree with the more precise breathing-zone single sensor, the results based on these sensors are likely less accurate [24]. While we aimed at creating a similar setting for each subject, there were minor variations in sitting positions and the angles between the breathing-zone of the subjects and the sensors, that might have influenced the accuracy of the particle measurements. The poor ability for the SPS30 sensor to separate particle sizes in bins [24] was a limitation for our ability to discern how different particle sizes propagate spatially.

Conclusion

In the study group of 20 healthy individuals, using HFNC and NIV did not lead to increased aerosol dispersal compared to low-flow oxygen treatment, except in rare cases. For a subject with non-productive cough, NIV with double-limb circuit and non-vented mask may be a favourable choice to reduce the risk for aerosol spread.

References

1. Demoule A, Vieillard Baron A, Darmon M, Beurton A, Geri G, Voiriot G, Dupont T, Zafrani L, Girodias L, Labbe V, Dres M, Fartoukh M, Azoulay E. High-Flow Nasal Cannula in Critically Ill Patients with Severe COVID-19. *Am J Respir Crit Care Med* 2020; 202(7): 1039-1042.
2. Mellado-Artigas R, Ferreyro BL, Angriman F, Hernandez-Sanz M, Arruti E, Torres A, Villar J, Brochard L, Ferrando C, Network C-SI. High-flow nasal oxygen in patients with COVID-19-associated acute respiratory failure. *Crit Care* 2021; 25(1): 58.
3. Tran K, Cimon K, Severn M, Pessoa-Silva CL, Conly J. Aerosol generating procedures and risk of transmission of acute respiratory infections to healthcare workers: a systematic review. *PLoS One* 2012; 7(4): e35797.
4. Jayaweera M, Perera H, Gunawardana B, Manatunge J. Transmission of COVID-19 virus by droplets and aerosols: A critical review on the unresolved dichotomy. *Environ Res* 2020; 188: 109819.
5. Zhang R, Li Y, Zhang AL, Wang Y, Molina MJ. Identifying airborne transmission as the dominant route for the spread of COVID-19. *Proc Natl Acad Sci U S A* 2020; 117(26): 14857-14863.
6. Smith SH, Somsen GA, van Rijn C, Kooij S, van der Hoek L, Bem RA, Bonn D. Aerosol persistence in relation to possible transmission of SARS-CoV-2. *Physics of Fluids* 2020; 32(10): 107108.
7. Iwashyna TJ, Boehman A, Capelcelatro J, Cohn AM, Cooke JM, Costa DK, Eakin RM, Prescott HC, Woolridge MS. Variation in Aerosol Production Across Oxygen Delivery Devices in Spontaneously Breathing Human Subjects. 2020.
8. Miller DC, Beamer P, Billheimer D, Subbian V, Sorooshian A, Campbell BS, Mosier JM. Aerosol Risk with Noninvasive Respiratory Support in Patients with COVID-19. *J Am Coll Emerg Physicians Open* 2020; 1(4): 521-526.
9. Takazono T, Yamamoto K, Okamoto R, Morimoto S, Izumikawa K, Mukae H. Effects of surgical masks on droplet dispersion under various oxygen delivery modalities. *Crit Care* 2021; 25(1): 89.
10. Leung CCH, Joynt GM, Gomersall CD, Wong WT, Lee A, Ling L, Chan PKS, Lui PCW, Tsoi PCY, Ling CM, Hui M. Comparison of high-flow nasal cannula versus oxygen face mask for environmental bacterial contamination in critically ill pneumonia patients: a randomized controlled crossover trial. *J Hosp Infect* 2019; 101(1): 84-87.
11. Gaekle NT, Lee J, Park Y, Kreykes G, Evans MD, Hogan CJ, Jr. Aerosol Generation from the Respiratory Tract with Various Modes of Oxygen Delivery. *Am J Respir Crit Care Med* 2020; 202(8): 1115-1124.
12. Li J, Fink JB, Ehrmann S. Author's Reply on High-Flow Nasal Cannula for COVID-19 Patients: Low Risk of Bio-Aerosol Dispersion. *Eur Respir J* 2020(56): 2003136.

13. Haymet A, Bassi GL, Fraser JF. Airborne spread of SARS-CoV-2 while using high-flow nasal cannula oxygen therapy: myth or reality? *Intensive care medicine* 2020; 46(12): 2248-2251.
14. Helgeson SA, Lee AS, Lim KG, Niven AS, Patel NM. Particulate generation with different oxygen delivery devices. *Respir Med* 2021; 181: 106386.
15. Wilson NM, Marks GB, Eckhardt A, Clarke AM, Young FP, Garden FL, Stewart W, Cook TM, Tovey ER. The effect of respiratory activity, non-invasive respiratory support and facemasks on aerosol generation and its relevance to COVID-19. *Anaesthesia* 2021.
16. Bem RA, van Mourik N, Klein-Blommert R, Spijkerman IJ, Kooij S, Bonn D, Vlaar AP. Risk of Aerosol Formation During High-Flow Nasal Cannula Treatment in Critically Ill Subjects. *Respir Care* 2021; 66(6): 891-896.
17. Li J, Fink JB, Elshafei AA, Stewart LM, Barbian HJ, Mirza SH, Al-Harthi L, Vines D, Ehrmann S. Placing a mask on COVID-19 patients during high-flow nasal cannula therapy reduces aerosol particle dispersion. *ERJ Open Res* 2021; 7(1).
18. Li J, Fink JB, Ehrmann S. High-flow nasal cannula for COVID-19 patients: risk of bio-aerosol dispersion. *Eur Respir J* 2020; 56(4).
19. Fennelly KP. Particle sizes of infectious aerosols: implications for infection control. *Lancet Respir Med* 2020; 8(9): 914-924.
20. Åkervik E, Fossum H, Dybwad M, Helgeland A. Airborne transmission of viral respiratory infections from an aerosol physics perspective. In: (FFI) NDRE, ed., FFI.no publications, 2020.
21. Jackson W. Nebulised Budesonide Therapy in Asthma: A Scientific and Practical Review Clinical Vision, 1995.
22. Hinds WC. Aerosol Technology: Properties, Behavior, and Measurement of Airborne Particles, 2nd Edition. Second edition ed. Wiley-Interscience, 1999.
23. Lindsley WG, Pearce TA, Hudnall JB, Davis KA, Davis SM, Fisher MA, Khakoo R, Palmer JE, Clark KE, Celik I, Coffey CC, Blachere FM, Beezhold DH. Quantity and size distribution of cough-generated aerosol particles produced by influenza patients during and after illness. *J Occup Environ Hyg* 2012; 9(7): 443-449.
24. Kuula J, Makela T, Aurela M, Teinila K, Varjonen S, Gonzalez O, Timonen H. Laboratory evaluation of particle-size selectivity of optical low-cost particulate matter sensors. *Atmos Meas Tech* 2020; 13(5): 2413-2423.

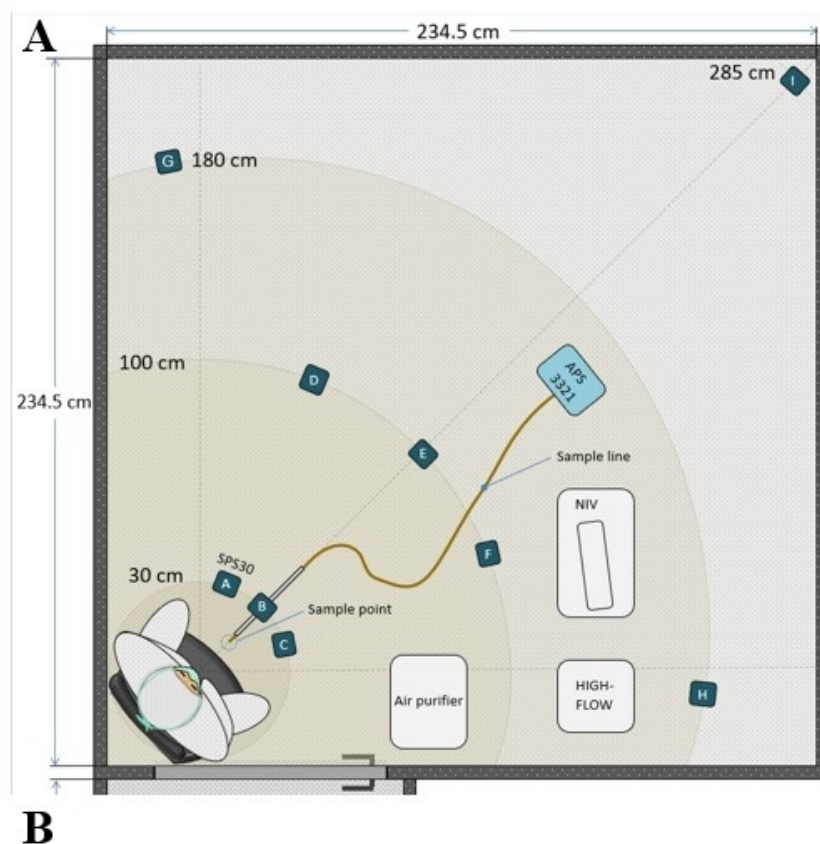


Figure 1. A) Overview of the test chamber, sensor locations (Sensirion, SPS30: mesh sensors: A-I, 3 sensors at 30 cm, 3 at 100 cm, 2 at 180 cm and 1 at 285 cm) (TSI, APS 3321: "breathing zone single sensor": sample point 20 cm from participant face) and other equipment. The test person was seated on a chair, with an approximate breathing zone elevation of 120 cm above the floor. The sensors were positioned 120 cm above the floor. B) Protocol structure with oxygen modalities and event elements and details. Before and between each 10-minute event a 15-minute period of filtering out the particles of the test chamber was performed.

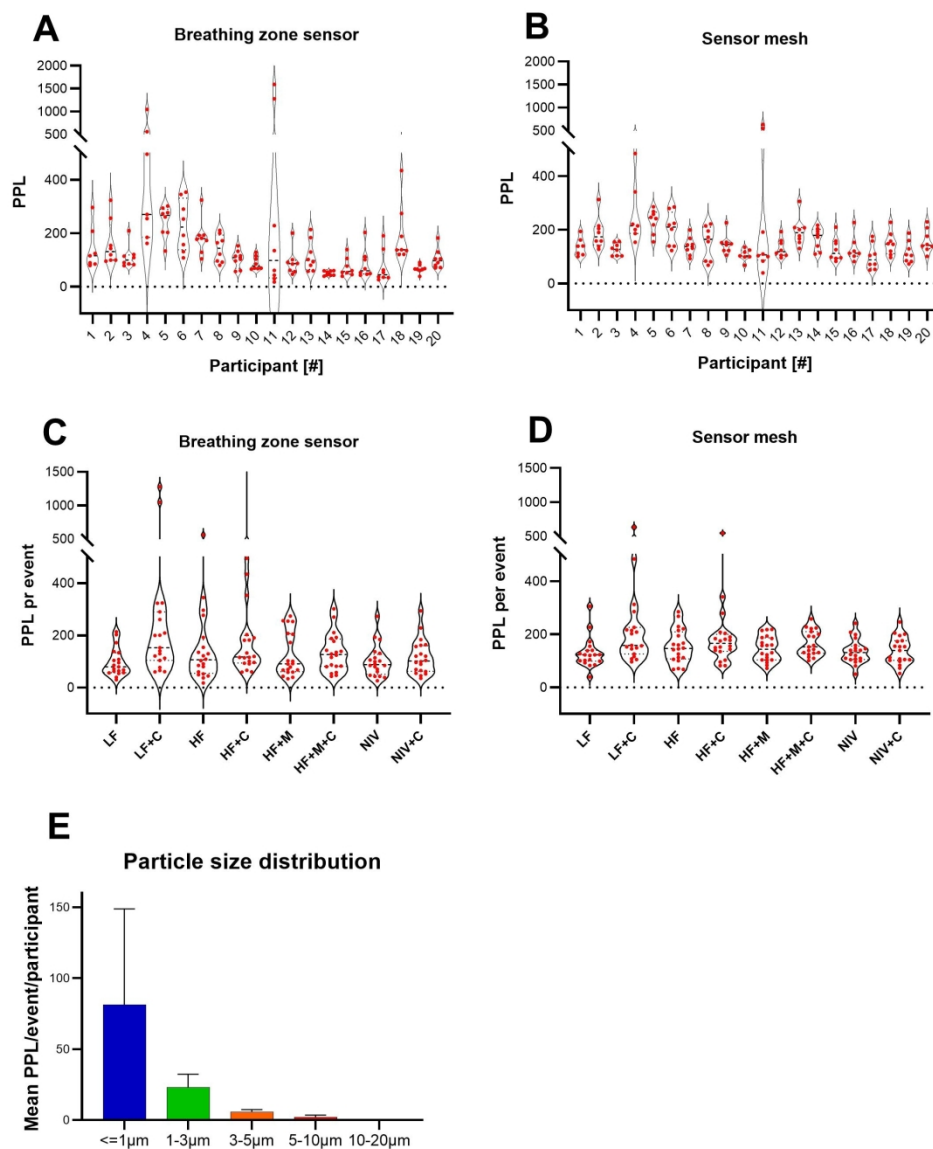


Figure 2. Top: Average Particles per litre of air (PPL) concentration over 10 minutes (red dot) between each of the eight events in each experiment, grouped according to participant (violin plots with two segment y-axes). A) breathing zone single sensor (particle size range 0.3 – 20 μm). B) average over nine mesh sensors (particle size range 0.3 – 10 μm). Bottom: Categorical comparisons of average concentration of particles per litres of air, during the eight events of each experiment, with each red dot representing the results from 1 of 20 participants, measured by the breathing zone single sensor (APS 3321) (C) and the average over all nine mesh sensors (D). The median is indicated with a thin black dashed line. Index of x-axis: LF= low-flow, C = cough, HF = high-flow, M = mask. E) Particle size distribution measured with the breathing zone sensor.

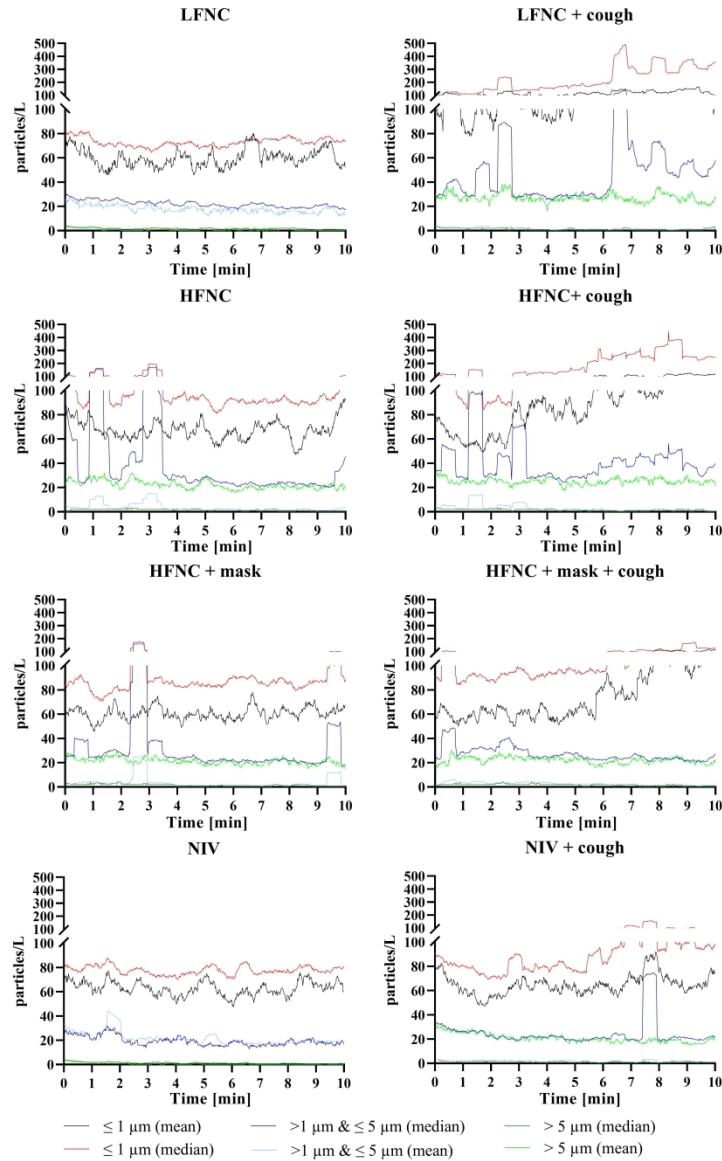


Figure 3. Mean and median particles per litre of air, from 20 participants, for three particle size groups, measured with the breathing zone single sensor (APS 3321), during the eight events of the experiment. The median and means show smoothed time series (moving mean with a 30 second window). The smoothing was used to increase readability and instead of a series of spikes, a smoothed square-like step response is shown for the periods with large spikes.

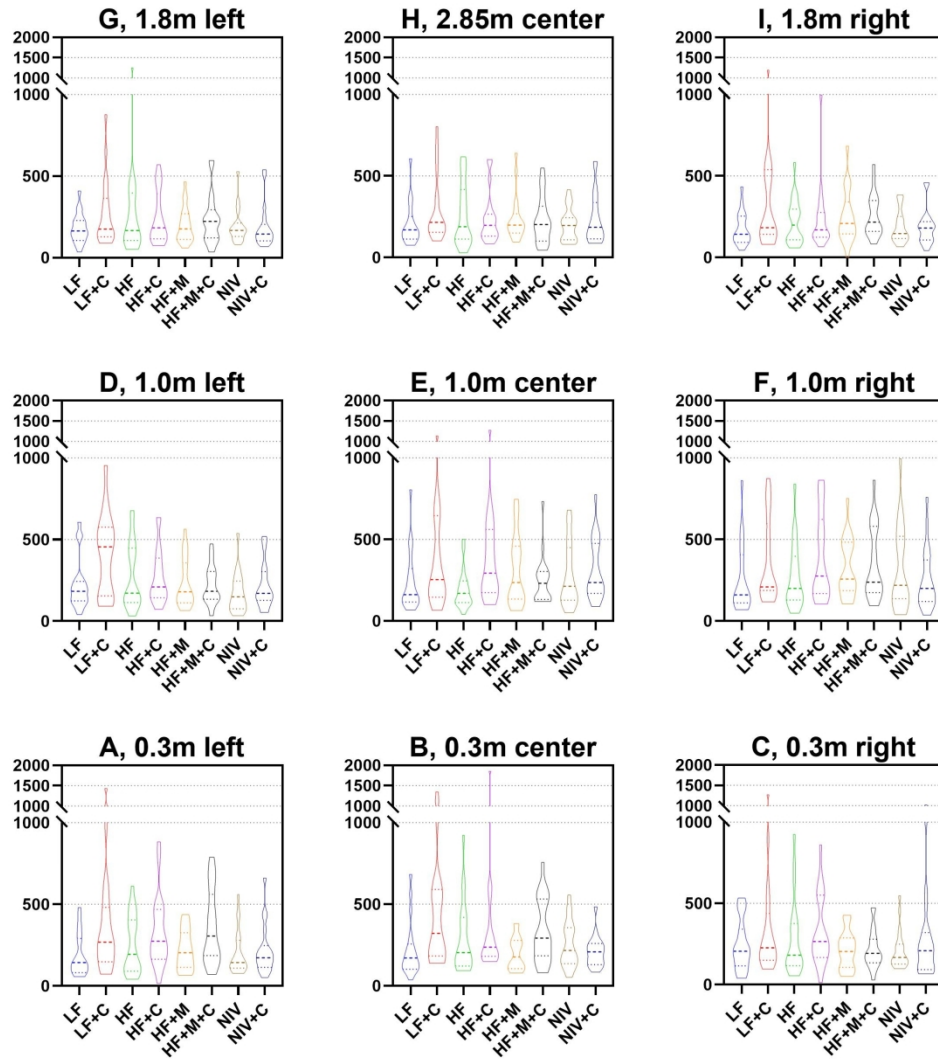


Figure 4. Mean particle concentration in particles per litre of air (y-axes) within each episode, for all mesh sensors. The particle concentration number includes particle sizes ($0.3 \mu\text{m}$ - $10 \mu\text{m}$). The placement of the plots within the graph is similar to the sensor position during the experiments, with the distance to each sensor shown in the subfigure headings. The distribution of measurements between participants is presented as violin plots, where the median is indicated with a thin black dashed line, and the quartiles with thinner dashed lines. Index of x-axis: LF= low-flow, C = cough, HF = high-flow, M = mask.

Online Data Supplement

Manuscript title:

Quantification of aerosol dispersal from suspected aerosol generating procedures

Authors:

Runar Strand-Amundsen, Christian Tronstad, Ole Elvebakk, Tormod Martinsen, Marius Dybwad, Egil Lingaas, Tor Inge Tønnessen

Tables

Table E1. *Statistical pairwise comparisons between different experimental episodes of particle concentrations for all mesh sensors in number concentration per litre. 95% confidence intervals of the median differences are based on the bootstrap method, and the p-values are based on the Wilcoxon signed rank test. LF = LFNC, HF = HFNC.*

Sensor	C					B					A				
	Comparison	Median diff	Lower CI	Upper CI	p-value	Median diff	Lower CI	Upper CI	p-value	Median diff	Lower CI	Upper CI	p-value		
Sensor	Comparison														
	HF - LF	15.2	-125.2	135.4	0.748	41.7	-53.8	131.4	0.314	8.2	-13.2	111.2	0.227		
	LF+cough - LF	19.9	-94.3	63.3	0.983	140.1	15.7	316.2	0.031	99.5	-15.3	206.5	0.064		
	HF+cough - HF	94.9	6.3	112.3	0.179	21.1	-51.9	128.2	0.313	104.3	-43.6	132.0	0.232		
	HF+cough - LF+cough	17.6	-50.2	114.5	0.573	-27.6	-194.8	49.7	0.227	-8.5	-131.6	58.1	0.445		
	HF - HF+mask	14.3	-54.9	108.6	0.313	55.3	-25.3	117.9	0.079	-23.1	-82.5	119.8	0.823		
	HF+cough - HF+mask+cough	51.7	-13.7	202.1	0.057	-14.8	-47.5	74.8	0.940	55.1	-149.4	106.9	0.911		
	HF+mask+cough - HF+mask	7.9	-22.7	44.5	0.709	72.9	23.2	210.3	0.005	125.2	-21.7	226.2	0.028		
	NIV - LF	2.7	-121.8	45.2	0.494	95.2	-42.7	142.3	0.277	-4.2	-82.9	40.2	0.778		
	NIV - HF	-13.5	-60.5	55.4	0.550	-10.5	-91.3	114.0	0.881	-31.2	-150.2	36.5	0.167		
	NIV+cough - NIV	4.7	-37.1	86.3	0.526	-14.7	-153.0	56.9	0.184	8.3	-26.9	61.6	0.575		
	LF+cough - NIV+cough	40.9	-25.9	53.1	0.184	123.5	33.8	345.3	0.001	63.8	20.8	128.4	0.044		
	HF+cough - NIV+cough	69.0	-8.0	182.2	0.145	69.1	-29.0	136.5	0.070	130.1	-15.4	231.5	0.126		
	F														
	Comparison														
	HF-LF	28.4	-110.7	145.1	0.629	0.5	-119.7	92.1	0.687	-7.2	-99.2	222.6	0.658		
	LF+cough - LF	62.4	-2.5	109.3	0.078	93.8	10.9	261.4	0.064	86.2	-6.5	338.9	0.039		
	HF+cough - HF	9.6	-55.1	276.4	0.232	97.7	53.9	204.0	0.004	9.4	-62.2	89.1	0.970		
	HF+cough - LF+cough	25.5	-23.3	94.5	0.355	51.9	-68.8	226.9	0.520	-35.5	-327.6	20.4	0.049		
	HF - HF+mask	-62.1	-199.4	34.3	0.247	-18.6	-313.8	46.0	0.117	15.6	-23.5	88.6	0.218		
	HF+cough - HF+mask+cough	-4.4	-41.1	121.9	0.852	27.3	-27.2	188.2	0.191	18.5	-24.8	90.6	0.204		
	HF+mask+cough - HF+mask	-49.7	-113.9	87.7	0.823	-55.8	-137.2	28.4	0.279	-10.6	-55.0	49.2	0.737		
	NIV - LF	18.2	-54.9	133.4	0.243	25.1	-56.7	127.6	0.520	-29.2	-81.1	2.8	0.212		
	NIV - HF	0.0	-50.1	164.2	0.627	17.8	-32.8	87.0	0.204	-64.0	-235.4	17.9	0.079		
	NIV+cough - NIV	-37.1	-169.7	35.6	0.247	60.1	-72.2	130.8	0.455	38.7	-24.3	105.9	0.156		
	LF+cough - NIV+cough	35.0	-19.2	133.6	0.049	-16.8	-59.3	122.6	0.872	184.8	28.8	401.6	0.027		
	HF+cough - NIV+cough	50.2	4.7	183.1	0.030	10.3	-49.6	132.1	0.433	44.6	-46.4	174.8	0.296		
	G														
Sensor	Comparison														
	HF-LF	43.6	-66.6	163.0	0.314	11.5	-22.4	46.6	0.355	13.7	-37.6	138.2	0.376		
	LF+cough - LF	40.9	-59.3	206.7	0.306	25.2	-25.9	118.5	0.306	38.7	-26.6	152.6	0.231		
	HF+cough - HF	10.4	-95.8	65.8	0.940	6.8	-73.2	57.5	0.794	-17.4	-61.8	37.8	0.526		
	HF+cough - LF+cough	-44.6	-195.7	21.3	0.084	-51.3	-132.0	-18.4	0.059	-54.3	-138.5	45.2	0.376		
	HF - HF+mask	-10.7	-93.5	26.9	0.526	23.8	-71.4	87.5	0.823	7.4	-65.8	111.3	0.627		
	HF+cough - HF+mask+cough	-29.9	-82.3	6.2	0.204	22.9	-42.2	94.7	0.658	8.7	-25.1	102.8	0.601		
	HF+mask+cough - HF+mask	20.7	-54.1	124.4	0.627	-11.7	-44.1	37.8	1.000	5.4	-33.4	116.3	0.455		
	NIV - LF	5.1	-93.8	56.9	0.904	29.0	-23.1	63.9	0.546	0.6	-53.1	54.8	0.809		
	NIV - HF	-8.9	-76.8	55.8	0.627	-18.2	-77.0	14.3	0.167	-47.9	-78.3	42.5	0.263		
	NIV+cough - NIV	-2.4	-60.3	77.8	0.970	14.9	-49.5	69.7	0.709	-24.5	-51.0	27.7	0.411		
	LF+cough - NIV+cough	18.1	-11.7	173.8	0.070	45.2	-42.7	125.4	0.212	35.6	-8.4	160.7	0.091		
	HF+cough - NIV+cough	22.0	-37.8	87.0	0.391	18.7	-45.9	89.3	0.654	38.1	-4.1	113.0	0.086		

Table E2. Estimates of change in particle concentration (number/litre) per minute for all episodes, based on the measurements from all mesh sensors. LF = LFNC, HF = HFNC.

Sensor	C				B				A			
Episode	Estimate	Lower CI	Upper CI	p-value	Estimate	Lower CI	Upper CI	p-value	Estimate	Lower CI	Upper CI	p-value
LF	2.7	-27.1	32.6	0.86	20.6	-5.5	46.8	0.12	7.7	-8.5	23.8	0.35
LF+cough	9.4	-33.3	52.1	0.66	42.5	-3.9	88.9	0.07	16.3	-27.6	60.3	0.46
HF	-7.7	-36.3	21.0	0.60	-6.3	-32.5	19.9	0.64	-27.9	-52.7	-3.0	0.03
HF+cough	14.4	-22.2	51.0	0.44	25.3	-23.3	74.0	0.31	6.5	-33.5	46.6	0.75
HF+mask	-2.9	-17.1	11.3	0.69	-7.5	-20.3	5.3	0.25	8.4	-4.0	20.8	0.18
HF+mask + cough	3.7	-7.3	14.7	0.51	-6.3	-40.8	28.2	0.72	13.6	-19.4	46.7	0.42
NIV	-1.0	-16.3	14.3	0.90	-1.5	-22.9	19.8	0.89	0.3	-10.1	10.6	0.96
NIV+ cough	-4.5	-35.0	26.1	0.77	-7.9	-20.6	4.8	0.22	10.2	-11.1	31.5	0.35

Sensor	F				E				D			
Episode	Estimate	Lower CI	Upper CI	p-value	Estimate	Lower CI	Upper CI	p-value	Estimate	Lower CI	Upper CI	p-value
LF	-12.3	-33.9	9.2	0.26	9.0	-22.6	40.7	0.57	-16.2	-41.8	9.3	0.21
LF+cough	27.2	-6.7	61.0	0.11	30.1	-15.5	75.7	0.19	22.9	-19.9	65.7	0.29
HF	-7.7	-26.0	10.6	0.41	-5.5	-14.0	2.9	0.20	-4.9	-27.9	18.1	0.68
HF+cough	26.5	-11.9	64.9	0.18	37.3	-12.1	86.7	0.14	15.8	-4.1	35.7	0.12
HF+mask	2.0	-37.5	41.4	0.92	20.1	-18.1	58.2	0.30	-3.5	-24.4	17.4	0.74
HF+mask + cough	12.6	-22.3	47.6	0.48	-5.7	-27.7	16.3	0.61	5.0	-10.1	20.0	0.52
NIV	-4.6	-35.9	26.8	0.77	-21.9	-57.4	13.6	0.23	-3.2	-14.8	8.3	0.58
NIV+ cough	-6.9	-33.1	19.2	0.60	2.3	-34.3	39.0	0.90	-7.1	-24.5	10.3	0.42

Sensor	H				I				G			
Episode	Estimate	Lower CI	Upper CI	p-value	Estimate	Lower CI	Upper CI	p-value	Estimate	Lower CI	Upper CI	p-value
LF	-5.6	-16.0	4.9	0.30	-7.6	-23.1	8.0	0.34	-9.4	-21.8	3.0	0.14
LF+cough	22.9	-7.0	52.8	0.13	21.3	-1.8	44.5	0.07	21.0	-9.2	51.1	0.17
HF	8.6	-11.3	28.5	0.39	12.9	-10.7	36.5	0.28	21.8	-1.2	44.8	0.06
HF+cough	19.7	-10.2	49.6	0.19	15.3	-4.9	35.5	0.14	9.6	-8.7	27.9	0.30
HF+mask	-1.4	-27.6	24.7	0.91	-2.3	-30.9	26.3	0.87	-8.9	-27.7	9.9	0.35
HF+mask + cough	-10.6	-31.9	10.7	0.33	7.3	-8.4	23.1	0.36	-0.4	-21.9	21.0	0.97
NIV	-7.3	-20.8	6.2	0.29	-6.0	-21.2	9.3	0.44	-8.0	-33.6	17.6	0.54
NIV+ cough	8.7	-2.3	19.8	0.12	-3.2	-30.0	23.5	0.81	-8.8	-25.2	7.6	0.29

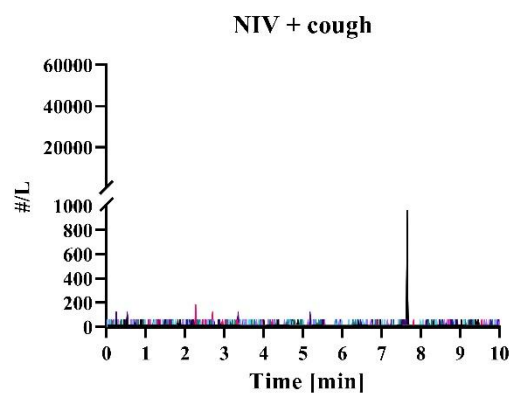
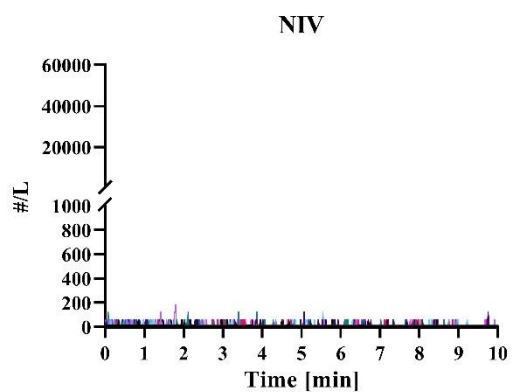
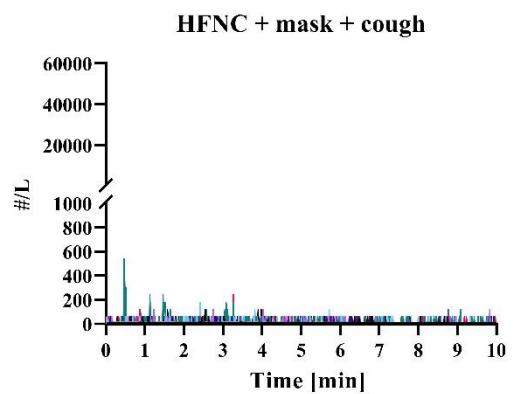
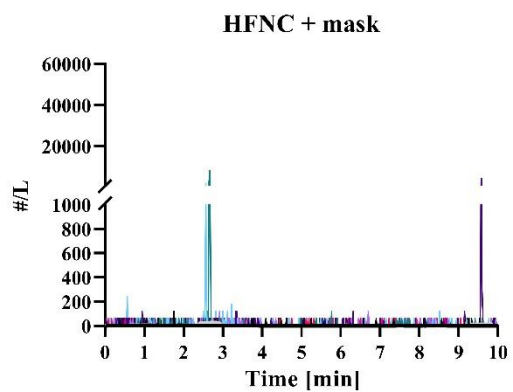
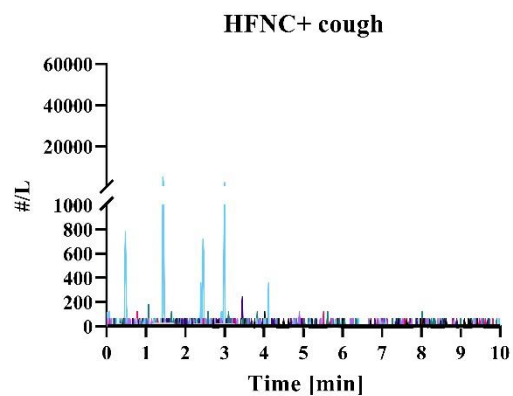
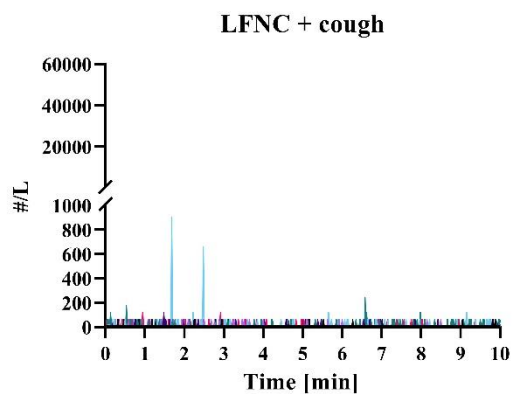
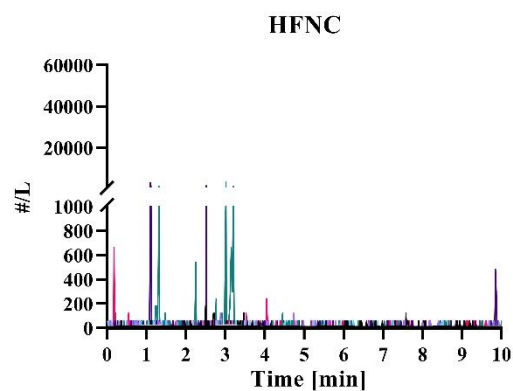
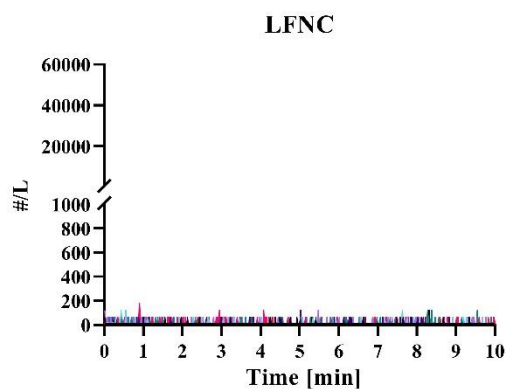


Figure E1. Raw data (particles per litre of air $>5\ \mu\text{m}$) from 20 participants measured with the breathing zone single sensor (APS 3321) for each of the 10-minute durations of the 8 episodes in the experiments. The black and grey lines show the median and mean respectively, of smoothed (moving mean with a 30 second window) time series from each experiment.

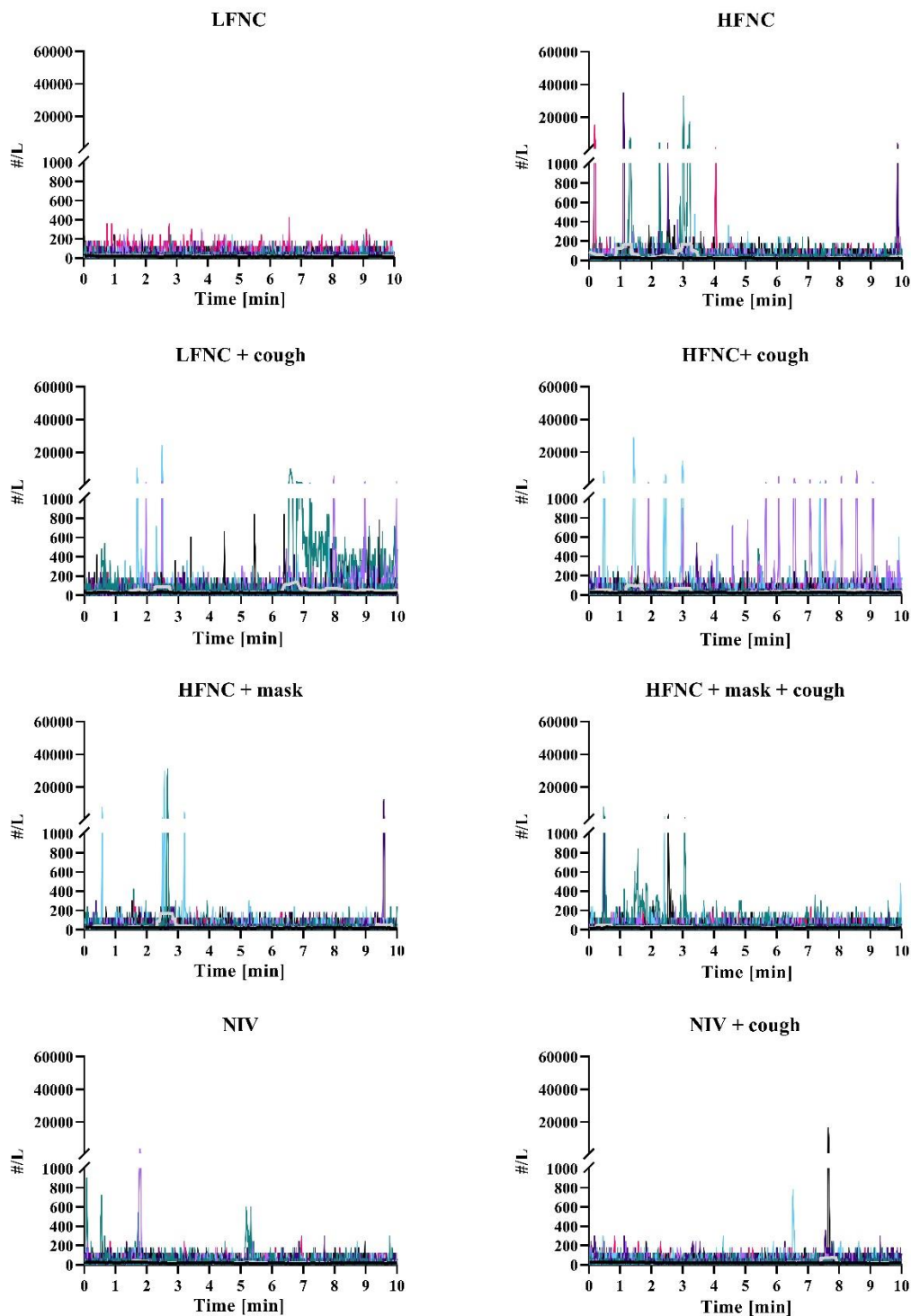


Figure E2. Raw data (particles per litre of air $> 1 \mu\text{m}$ & $\leq 5 \mu\text{m}$) from 20 participants measured with the breathing zone single sensor (APS 3321) for each of the 10-minute durations of the 8 episodes in the experiments. The black and grey lines show the median and mean respectively, of smoothed (moving mean with a 30 second window) time series from each experiment.

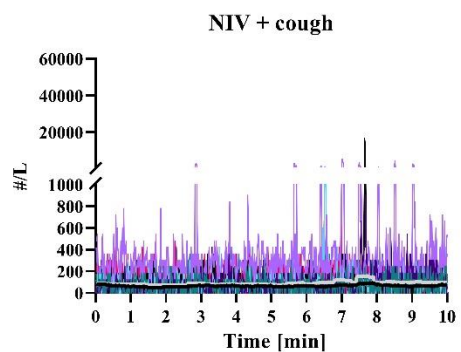
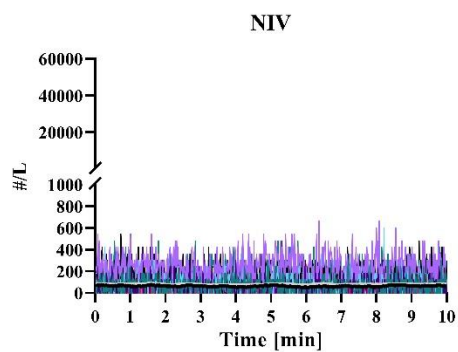
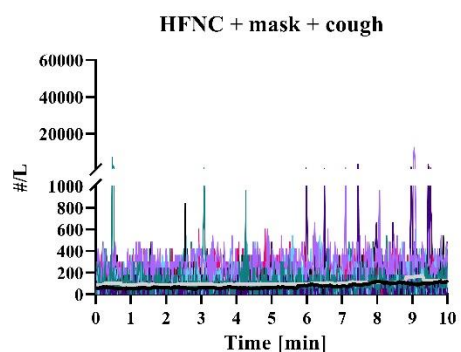
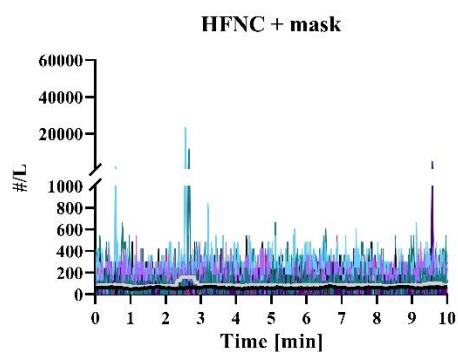
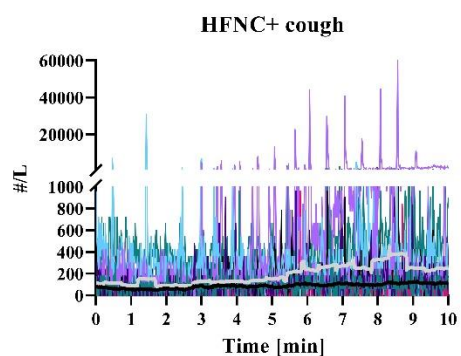
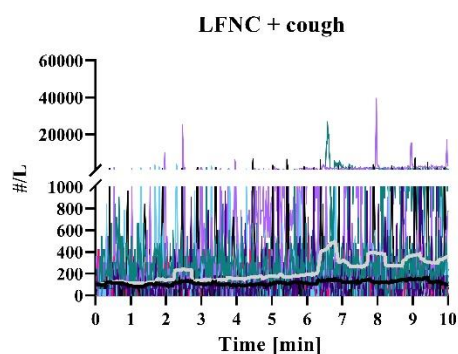
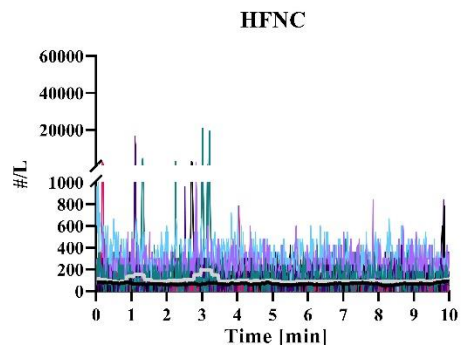
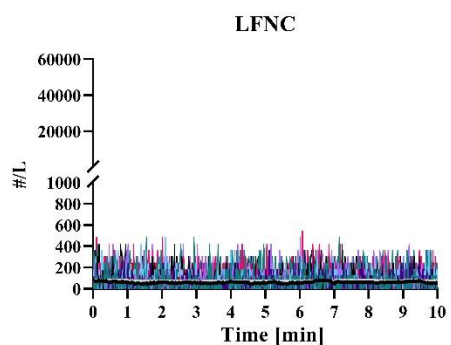


Figure E3. Raw data (particles per litre of air $\leq 1.0 \mu\text{m}$) from 20 participants measured with the breathing zone single sensor (APS 3321) for each of the 10-minute durations of the 8 episodes in the experiments. The black and grey lines show the median and mean respectively, of smoothed (moving mean with a 30 second window) time series from each experiment.